European Spine Journal

Staying connected: structural integration at the intervertebral disc-vertebra interface of human lumbar spines

Sharon Brown, Samantha Rodrigues*, Christopher Sharp[ǂ], Kelly Wade*, Neil Broom*, Iain W McCall, Sally Roberts

Spinal Studies, RJAH Orthopaedic Hospital Foundation Trust & ISTM (Keele University), Oswestry, Shropshire, UK

*Dept of Chemical & Materials Engineering, University of Auckland, Auckland, New Zealand

[ǂ]Institute of Medicine, University Centre Shrewsbury, University of Chester, Shrewsbury, Shropshire, UK

Corresponding author: Sharon Brown

Sharon.owen@rjah.nhs.uk

Tel: +44 1691 404660

Acknowledgements: This study was supported by the Orthopaedic Institute Ltd, Robert Jones & Agnes Hunt Orthopaedic Hospital, Oswestry and a Travelling Fellowship from the Winston Churchill Memorial Trust (Sharon Owen (nee Brown)). We are grateful to Mike Haddaway and Dr Victor Cassar-Pullicino and members of the Imaging Department for their support.

Abstract

Purpose:

To investigate the microscopic fibrous integration between the intervertebral disc, cartilage endplates and vertebral endplates in human lumbar spines of varying degrees of degeneration using differential interference contrast (DIC) optics. Weakness at these junctions is considered to be an important factor in the aetiology of disc herniations.

Methods:

Magnetic resonance images (MRIs) of cadaveric lumbar spines were graded for degeneration and motion segments from a range of degenerative grades isolated and bisected sagittally. Following fixation and decalcification, these were cut into segments containing anterior or posterior annulus fibrosus or nucleus pulposus. The segments were cryo-sectioned and sections visualised using both standard light and DIC microscopy.

Results:

Detachment at the interface between the disc and vertebrae increased with greater degenerative grade (from 1.9% in Grade I to 28% in Grade V), especially at the boundary between the cartilage and vertebral endplates. DIC microscopy revealed the fibrous organisation at the IVD-cartilage endplate interface with structural features, such as annular lamellae branching and nodal insertions in the nucleus pulposus region; these have been previously observed in ovine spines, but were less uniform in humans. Structural integrity of the IVD and cartilage endplate was also lost with increasing degeneration.

Conclusions:

This preliminary study shows that microscopic structural features may act to maintain attachment between the IVD and CEP in the human spine. Loss of structural integrity in this region may destabilise the spine, possibly altering the mechanical environment of the cells in the disc and so potentially contribute to the aetiopathogenesis of IVD degeneration.

Keywords 4-6: Differential interference contrast (DIC) microscopy; lamellae branching; nodal insertions; collagen; degeneration

Introduction

The cartilage (CEP) and vertebral (VEP) endplates play a crucial structural role in the transition from hard, bony vertebrae to compliant intervertebral disc (IVD) tissue and enable force transmission and movement within the spine [10]. Both endplates have load-bearing functions and prevent the IVD from entering the vertebrae [7], and in humans, is involved in vertebral growth [32]. The VEP, with its relatively thick epiphyseal ring at the outer margin in the adult spine, where there is no CEP, is thinner and more porous in the centre [39], [40]; similarly the depth of the CEP becomes narrower towards its centre [27], [19]. Although this central region is important for nutrient diffusion from the vascularised bone to the avascular nucleus pulposus, its properties (at least for the VEP) have been shown to be closely related to local mechanical loading [43]. The integrity of both of these endplates is necessary for IVD maintenance [26], [5], [40].

Failure at the interface between the IVD and VEP appears to be a main contributor in the aetiology of herniations [33], [25], [38], with endplate being present in almost 50% of herniated disc tissue [20], but structural integrity at this junction has not previously been investigated in the aetiology of disc degeneration Several studies report clear integration between the IVD and CEP, with collagen fibres running seamlessly between the two tissues [17], [13], [12], [27]; a recent study by Herrero *et al* [11] focussed on non-degenerate human spines and showed that integration at the CEP-VEP junction changes with age and with spinal level. It is well recognised that, at the outer annulus fibrosus (AF), fibres are continuous from the IVD to the VEP [14], but integration at the CEP-VEP interface remains questionable, with some proposing that it is present [12] and others that it is not [27], [13].

A specialised form of microscopy using differential interference contrast (DIC) optics has been used to determine the microscopic, fibrous organisation at the interfaces between the AF-CEP [29], NP-CEP [34], [35] and NP-AF [36] in sheep. This technique enables the visualisation of tissues containing a range of fibre orientations with increased resolution and clarity compared with standard light microscopy, and has been instrumental in the identification of annular lamellae sub-branching at the AF-CEP junction [29] and the presence of nodal insertions at the NP-CEP junction [34] in sheep.

In the present preliminary study, we have investigated how the IVD connects across the endplates in *human* lumbar vertebral motion segments. We have measured the degree to which the IVD is detached from the endplates and related this to the Pfirrmann degenerative grade. We have recorded the organisation of IVD fibre integration into the endplates via DIC microscopy and noted detrimental changes to the CEP and IVD. Finally, alterations in structure were considered in relation to MRI findings.

Methods

Clinical imaging and Pfirrmann grading of cadaveric lumbar spines

Six, intact, frozen post-mortem lumbar spines from anonymous donors were imaged using standard clinical-grade X-ray (Fig. 1) and MR imaging. MRI was performed with a Siemens ‘Skyra’ 3T machine, running version VD1 software and utilised both T1

and T2 weighted sequences (TSE–Turbo spin echo). Images were assessed by a consultant radiologist (IWM) and graded for degeneration using the Pfirrmann classification system (Grade I (normal) to Grade V (extensive degeneration)) based on distribution and intensity of signal from the IVD, clear visualisation of the NP and AF and loss of IVD height [24]. Additional criteria described by Battié *et al* [4] were also noted including assessing the presence of spondylolisthesis, annular tears, disc bulging, degree and location of herniations, endplate defects and sclerosis and facet joint arthropathy (Table 1).

Specimen preparation for DIC optical microscopy

Ten motion segments representing a range of Pfirrmann grades (I – V) were isolated via transverse cuts through the centre of adjacent vertebral bodies from lumbar regions L1-5 (Table 1) and cut sagittally (Fig. 1). The right-hand side of the specimen was fixed in 10% formalin at 4°C and decalcified in 10% formic acid before dissecting along the coronal axis to generate segments containing either the anterior or posterior AF or NP (Fig. 2). AF containing segments were cryo-sectioned obliquely at 30 µm along an exposed outer lamellar bundle to enable visualisation of both in-plane and cross-sectional annular fibres [30] and NP containing segments were cryo-sectioned either along the sagittal (n=8) or coronal axis (n=2). All sections were wet mounted onto slides in PBS and examined using standard light and DIC optical microscopy.

Analysis of microscopic images

Using standard light microscopy, each section was imaged and the length of the interfaces between the VEP-AF, VEP-CEP, CEP-AF and CEP-NP was measured. Any loss of attachment between each individual interface was recorded then combined to generate an average percentage detachment for the disc-vertebral body interface of each motion segment, in addition to an overall detachment (%) for each interface region (CEP-VEP, IVD-VEP and IVD-CEP) for all the motion segments studied (Table 2, data presented as mean ± SD).

The organization of the collagenous fibres at the VEP-AF, CEP-AF and CEP-NP were visualised via DIC microscopy and recorded. The structural integrity of the AF and NP was assessed separately using a scoring system where 1 = no disruption, 2 = minor, 3 = moderate, and 4 = major disruption, as illustrated for the AF in Fig. 3, and the scores were added to generate an IVD score. Degeneration of the CEP was assessed using the classification system derived by Boos *et al* [6]. This system scores features such as bony sclerosis, new bone formation and micro-fracture from 0 to 2, and cartilage cracks, cartilage disorganisation and cellularity from 0 to 4, with higher scores reflecting increased degeneration.

Results

Pfirrmann grading of specimens from MRI

The degenerative features observed in the specimens studied are summarised in Table 1. Both Pfirrmann grade I specimens had a normal disc height and contour and contained no annular tears, foraminal stenosis or endplate defects. The six Grade III specimens had no disc narrowing or foraminal stenosis, but an annular tear was present in two specimens with one also having anterior and posterior disc bulging. Endplate defects were present in two other specimens, in which vertebral collapse had occurred due to osteoporosis, with one of these also having both anterior and posterior disc bulging. In the Grade IV specimen there was slight disc narrowing and bulging at the posterior AF, whilst the Grade V specimen had a severely narrowed disc with slight to moderate disc bulging, mild foraminal stenosis and generalised endplate irregularities and osteophytes at both anterior and posterior regions.

Detachment at the IVD-vertebra interface is associated with Pfirrmann degenerative grade

Although detachment was variable in the different regions of the IVD-vertebra interface for each specimen (Table 2), there was a trend for the percentage detachment across the whole disc-vertebra interface to increase with Pfirrmann grade (I = 1.9 ± 2.7%; III = 16.9 ± 10.2%; IV = 21.3%; V = 28%) (Fig. 4a & b). Additionally, detachment was greater at the CEP-VEP interface (29.5 ± 33.2%) than either the IVD-VEP (5.3 ± 9.9%) or IVD-CEP (8.0 ± 12.9%) interfaces (Table 2) when the data from all specimens was combined. The percentage of detachment was also greater at the cranial (relative to the IVD) CEP-NP than the caudal interface. In some degenerate specimens, it was not possible to measure the interfaces.

Microscopic organisation and structure at the IVD-vertebra interface

(i) The AF-vertebra interface

Generally there was good integration at the AF-vertebra interface, especially in Pfirrmann grade I (Fig. 5a) where lamellar organisation was similar to that previously observed in sheep (Fig. 5b); however, in humans, the lamellae were not as uniform or as evenly distributed (Fig. 5a). In the human specimens, there was less obvious crimp (the wave-like appearance commonly seen in ligaments, representing closely packed collagen fibrils that are in phase and relaxed) and a change in optical density (OD) observed in collagen fibres of the outer AF lamellae (Fig. 6a & b) before they entered the bony VEP. This loss in crimp and change in OD is suggestive of calcification, and is similar to the AF-CEP interface in sheep (Fig. 6c & d) where there was no crimp in the AF fibres entering the more rigid calcified CEP [29]. In contrast, at the AF-CEP junction in humans, crimp was present in the AF fibres where they integrated with the CEP, although their appearance seemed to change from a wider to a narrower crimp, that is, the 'banding' visible in the tissue from the in-phase collagen fibrils are closer together (Fig. 7). Additional features observed in some human specimens included: branching of lamellae at the AF-CEP interface, where the collagen fibres appear to continue into the CEP (Fig. 8a); trans-lamellar bridges [23], where fibrous connections span many lamellae (Fig. 8b), and compartmentalisation [41], where the AF collagen fibre bundles appear to be ensheathed (Fig. 8c).

(ii) The CEP-VEP interface

There was little evidence of collagen fibres crossing the junction between the CEP and VEP when viewed with DIC. Indeed the boundary between these two endplates usually appeared uneven (Fig. 9) with the two structures appearing to interlock with each other.

(iii) The NP-CEP interface

In general, detachment at the NP-CEP interface increased with increasing degenerative grade, although some Pfirrmann grade III specimens had good attachment (Table 2). Nodal insertions, previously described in sheep by Wade *et al* [34], [35], where fibres from the NP are clearly seen to insert into the CEP at discrete locations, were also observed in the human lumbar specimens (Fig. 10a & b). In contrast to those observed in sheep (Fig. 10c), these insertions in human specimens were not as regular or as evenly distributed. Generally, when there was good attachment between the NP and CEP, the fibres of the NP at this junction were orientated perpendicularly to the CEP interface (Fig. 10a, b & d) and had a 'wave-like' morphology (Fig. 10d).

Structural and degenerative changes in the IVD and CEP in relation to Pfirrmann degenerative grade

Higher IVD integrity scores (ie reflecting more disruption and diminished structural cohesion and organisation within the IVD determined from both the NP and AF) were found in discs of greater Pfirrmann degenerative grades (I = 2.75 ± 1.1; III = 5.4 ± 0.9; IV = 5.5). No IVD score is presented for the Grade V specimen as the AF could not be obliquely sectioned; however the NP of this specimen had major structural disruption and scored 4. Similarly, elevated scores (reflecting degenerative changes) for the CEP were found with higher Pfirrmann degenerative grades (I = 4.3 ± 2.2; III = 6.9 ± 3.5; IV = 7.5 ± 6.4; V = 13.5 ± 0.7).

Microscopic structure in relation to MRIs and Pfirrmann degenerate grade

Perhaps not surprisingly, there appeared to be an association between the Pfirrmann grade and the level of disruption and other microscopic degenerative features visible microscopically. Both specimens which were described as Grade I Pfirrmann from their MRI appearance had a well organised AF and intact NP at the microscopic level, whereas in more degenerate specimens with a higher Pfirrmann grade, with loss of signal intensity and lack of distinction between the AF and NP, the AF could be seen to be more disorganised and the NP very disrupted when examined under the microscope. In three specimens (all Grade III), annular tears were seen when studied under the microscope, but only one corresponded to a tear visualised on MRI. Disc bulging was also detected by MRI in three specimens and in all these specimens the fibre direction at the IVD-CEP junction was not perpendicular to the CEP, as observed in Grade I specimens at this interface, but rather was more oblique.

Discussion

Our preliminary findings suggest that lack of integration, especially at the CEP-VEP interface, is associated with IVD degeneration and adds to the current knowledge within the field, whereby lack of structural integrity at the CEP-VEP junction is increasingly being implicated in the aetiology of herniations [31], [20], [40], [16], [3]. Possible reasons for reduced connectivity at the CEP-VEP junction may be either an increase in marrow spaces abutting this interface [18], so reducing locations where fibre integration is possible or retention of discontinuities in the endplate following insufficient retraction of the notochord during spinal development [8]. A further reason could be due to actual physical disruption, as has been described in a recent biomechanical study in which the IVD was subjected to loading in tension such as might be experienced during spinal bending [3]. Indeed, the mechanism by which these two tissues are secured together may be more reliant on the rigid inorganic fraction present in the tissues instead of the soft non-mineralised organic fraction. Paietta *et al* [22] suggest that the calcified cartilage and underlying bone interdigitate with one another; if this occurs 3-dimensionally, one can imagine it would allow interlocking of the two mineralised regions. The structural integration of collagen at the AF-VEP junction however, remains an understudied area in the human spine, but ultrastructural imaging techniques, as utilised recently by Rodrigues *et al* [28] in combination with DIC images have provided an insight into the organisation of AF "sub-bundle fibrils" in sheep. They have shown that these fibrils penetrate beyond the cement line and merge with those present in both the CEP and VEP. This work has been performed in sheep, where it is known that, as in other animal species, the growth plate for the vertebrae is located within the centre of the vertebral body [1]; in contrast to in humans where it is an integral part of the CEP. The effect of growth plate location and the degeneration process on collagen integration at the CEP-VEP interface thus remains unclear.

From our data, the degree of detachment in the Pfirrmann Grade III specimens was usually greater than 10%, but in one specimen it was as low as 2%. This specimen was one in which some interfaces were not measurable due to the presence of severe endplate sclerosis (also noted in another Grade III and the Grade V specimen, Table 2) and it is highly likely that in these specimens the degree of detachment would actually have been higher if they could have been measured.

Better connectivity was observed at the IVD-VEP and IVD-CEP junctions than between the CEP and VEP where, at the IVD-CEP interface in particular, good fibre integration was seen, concurring with previous findings at these interfaces [17], [13], [12], [27]. Due to the presence of the epiphyseal ring in human spines, there are fibres from the outer AF continuing into the VEP, whilst those at the inner AF continue into the CEP. Good connectivity was observed at both these interfaces in most specimens, but particularly at the AF-CEP where 7/9 and 5/7 specimens showed no detachment at the anterior and posterior disc, respectively. However, in comparison to sheep, the AF lamellae in these human specimens were not as uniformly distributed, but branching of individual, in-plane AF lamellae was observed at the AF-CEP interface, similar to that seen in the ovine spine [29] and in herniated human IVDs [15]. This mechanism increases the attachment area between the two structures and is likely to enhance the tensile stress that can be sustained at this junction helping to resist detachment. Additionally, at the AF-CEP interface, crimp

was visible within the AF collagen fibres, whereas at the AF-VEP junction crimp was lost just prior to anchorage into the bony VEP, indicating that this region was previously calcified. It should be noted that the crimp morphology confers on the annular fibres a considerable degree of flexibility that would have no functional value in terms of contributing to the strength of anchorage once embedded in the rigid substrate of the CEP. It has been shown in previous studies [28], [29] that this abrupt change in the collagen fibre morphology from a crimped to a non-crimped configuration provides an effective visual marker of the exact boundary between the fibres in their flexible versus rigid or embedded state when viewed in sections that have been obtained from decalcified specimens. This intermediary zone between the AF and vertebra may be similar to the calcified cartilage found below articular cartilage and is probably important not only for attaching the fibres to the mineralised bone of the vertebrae, but also mechanically, to assist the transfer of forces between the hard mineralised bony VEP and the un-mineralised disc [21].

At the NP-CEP interface, the collagen fibres of the NP were usually orientated perpendicularly to the CEP, although in some cases, especially where bulging of the disc was seen on clinical imaging, they entered at a more oblique angle. The presence of nodal insertions, (ie discrete locations at which the collagen fibres of the NP insert into the CEP), were visible in both Grade I and some of the more degenerate specimens. Nodal insertions have previously been described in sheep [34], [35], where they were found to be evenly distributed across the NP-CEP interface and were particularly visible when the disc was loaded under tension [34], although in mature sheep they become less distinct [37]. Since our motion segments were from adult cadavers that had not been loaded under tension, the nodal insertions may have been more difficult to identify.

As expected, the structural integrity and organisation within the IVD and CEP was found to decrease with increasing Pfirrmann degenerative grade. Although MRI has been successful in diagnosing later stages of IVD degeneration, early degenerative changes in the disc matrix, even with enhanced MRI, only correlate moderately with tissue histology [9]. In the present study, some histological and microscopic features, such as fibre angle changes at the IVD-CEP junction and loss of disc integrity, appeared to reflect the disc bulging and change in signal and loss of AF and NP distinction observed on the MRIs. In particular, loss of structure at the AF and NP junction, which has previously been shown to be capable of supporting considerable loads in sheep [36], warrants further investigation in the human spine, as well as the role of other structural elements, such as elastin at this interface [42]. The degenerative changes seen in the CEP have been well characterised and shown to be associated with IVD degeneration [2]; they will inevitably impinge on the state of connectivity at the disc and vertebra interfaces. Lama *et al* [16] have highlighted that any loss in CEP will result in increased endplate permeability thus possibly facilitating endplate inflammation or even disc infection which may subsequently play a role in the generation of Modic changes as observed on MRI.

This study is the first to use DIC for analysis of the fibrous structure at the interfaces between the IVD and vertebral bodies in a small number of human spines containing IVDs of varying degrees of degeneration. There are of course limitations within the study, one being that the number of cadaveric specimens investigated is small and so no statistical analysis could be undertaken. In addition, since these lumbar spines were an historic collection obtained anonymously and thus patient details were

not known for all of the donors, we were unable to take into account factors such as age or gender; the MRIs from which the degenerative grades were determined, however, are recent and hence reflect the current tissue degenerative state. Whilst detachment at the interfaces was carefully assessed to ensure that they resembled 'naturally' occurring clefts, it must be noted that the sampling and histological processing may have introduced artefacts within these tissues.

Conclusion

Hence, in conclusion, we have shown that microscopic structural features, such as lamellar branching and nodal insertions, may act to maintain attachment between the IVD and CEP in the human spine. Loss of structural integrity at the disc-vertebra junction may not only destabilise the spine at that point, but could alter the mechanical environment of the cells, not only at this junction, but also possibly within the disc, and so potentially contribute to the aetiopathogenesis of IVD degeneration.

References

1. Alini M, Eisenstein SM, Ito K, Little C, Kettler AA, Masuda K, Melrose J, Ralphs J, Stokes I, Wilke HJ (2008) Are animal models useful for studying human disc disorders/degeneration? Eur Spine J 17:2-19

2. Aoki J, Yamamoto I, Kitamura N, Sone T, Itoh H, Torizuka K, Takasu K (1987) End plate of the discovertebral joint: degenerative change in the elderly adult. Radiology 164:411-414

3. Balkovec C, Adams MA, Dolan P, McGill SM (2015) Annulus Fibrosus Can Strip Hyaline Cartilage End Plate from Subchondral Bone: A Study of the Intervertebral Disk in Tension. Global Spine J 5:360-365

4. Battie MC, Lazary A , Fairbank J, Eisenstein S, Heywood C, Brayda-Bruno M, Varga PP, McCall I (2014) Disc degeneration-related clinical phenotypes. Eur Spine J 23 Suppl 3:S305-S314

5. Benneker LM, Heini PF, Alini M, Anderson SE, Ito K (2005) 2004 Young Investigator Award Winner: vertebral endplate marrow contact channel occlusions and intervertebral disc degeneration. Spine (Phila Pa 1976) 30:167-173

6. Boos N, Weissbach S , Rohrbach H, Weiler C, Spratt KF, Nerlich AG (2002) Classification of age-related changes in lumbar intervertebral discs: 2002 Volvo Award in basic science. Spine 27 :2631-2644

7. Broberg KB (1983) On the mechanical behaviour of intervertebral discs. Spine (Phila Pa 1976) 8:151-165

8. Corsi A, De Maio F, Mancini F, Ippolito E, Riminucci M, Bianco P (2008) Notochordal inclusions in the vertebral bone marrow. J Bone Miner Res 23:572-575

9. Detiger SE, Holewijn RM, Hoogendoorn RJ, van Royen BJ, Helder MN, Berger FH, Kuijer JP, Smit TH (2014) MRI T2* mapping correlates with biochemistry and histology in intervertebral disc degeneration in a large animal model. Eur Spine J

10. Ferguson SJ,Steffen T (2003) Biomechanics of the aging spine. Eur Spine J 12 Suppl 2:S97-S103

11. Herrero CF, Garcia SB, Garcia LV, Aparecido Defino HL (2014) Endplates changes related to age and vertebral segment. Biomed Res Int 2014:545017

12. Humzah MD,Soames RW (1988) Human intervertebral disc: structure and function. Anat Rec 220:337-356

13. Inoue H (1981) Three-dimensional architecture of lumbar intervertebral discs. Spine (Phila Pa 1976) 6:139-146

14. Johnson EF, Chetty K, Moore IM, Stewart A, Jones W (1982) The distribution and arrangement of elastic fibres in the intervertebral disc of the adult human. J Anat 135:301-309

15. Junhui L, Zhengfeng M, Zhi S, Mamuti M, Lu H, Shunwu F, Fengdong Z (2015) Anchorage of annulus fibrosus within the vertebral endplate with reference to disc herniation. Microsc Res Tech 78:754-760

16. Lama P, Zehra U, Balkovec C, Claireaux HA, Flower L, Harding IJ, Dolan P, Adams MA (2014) Significance of cartilage endplate within herniated disc tissue. Eur Spine J 23:1869-1877

17. Maroudas A, Stockwell RA, Nachemson A, Urban J (1975) Factors involved in the nutrition of the human lumbar intervertebral disc: cellularity and diffusion of glucose in vitro. J Anat 120:113-130

18. McFadden KD,Taylor JR (1989) End-plate lesions of the lumbar spine. Spine (Phila Pa 1976) 14:867-869

19. Moon SM, Yoder JH, Wright AC, Smith LJ, Vresilovic EJ, Elliott DM (2013) Evaluation of intervertebral disc cartilaginous endplate structure using magnetic resonance imaging. Eur Spine J 22:1820-1828

20. Moore RJ, Vernon-Roberts B, Fraser RD, Osti OL, Schembri M (1996) The origin and fate of herniated lumbar intervertebral disc tissue. Spine 21:2149-2155

21. Nosikova YS, Santerre JP, Grynpas M, Gibson G, Kandel RA (2012) Characterization of the annulus fibrosus-vertebral body interface: identification of new structural features. J Anat 221:577-589

22. Paietta RC, Burger EL, Ferguson VL (2013) Mineralization and collagen orientation throughout aging at the vertebral endplate in the human lumbar spine. J Struct Biol 184:310-320

23. Pezowicz CA, Robertson PA, Broom ND (2006) The structural basis of interlamellar cohesion in the intervertebral disc wall. J Anat 208:317-330

24. Pfirrmann CW, Metzdorf A, Zanetti M, Hodler J, Boos N (2001) Magnetic resonance classification of lumbar intervertebral disc degeneration. Spine (Phila Pa 1976) 26:1873-1878

25. Rajasekaran S, Bajaj N, Tubaki V, Kanna RM, Shetty AP (2013) ISSLS Prize winner: The anatomy of failure in lumbar disc herniation: an in vivo, multimodal, prospective study of 181 subjects. Spine (Phila Pa 1976) 38:1491-1500

26. Roberts S, Menage J, Eisenstein SM (1993) The cartilage end-plate and intervertebral disc in scoliosis: calcification and other sequelae. J Orthop Res 11:747-757

27. Roberts S, Menage J, Urban JP (1989) Biochemical and structural properties of the cartilage end-plate and its relation to the intervertebral disc. Spine (Phila Pa 1976) 14:166-174

28. Rodrigues SA, Thambyah A, Broom ND (2015) A multiscale structural investigation of the annulus-endplate anchorage system and its mechanisms of failure. Spine J 15:405-416

29. Rodrigues SA, Wade KR, Thambyah A, Broom ND (2012) Micromechanics of annulus-end plate integration in the intervertebral disc. Spine J 12:143-150

30. Schollum ML, Robertson PA, Broom ND (2009) A microstructural investigation of intervertebral disc lamellar connectivity: detailed analysis of the translamellar bridges. J Anat 214:805-816

31. Tanaka M, Nakahara S, Inoue H (1993) A pathologic study of discs in the elderly. Separation between the cartilaginous endplate and the vertebral body. Spine (Phila Pa 1976) 18:1456-1462

32. Taylor JR (1975) Growth of human intervertebral discs and vertebral bodies. J Anat 120:49-68

33. Veres SP, Robertson PA, Broom ND (2009) The morphology of acute disc herniation: a clinically relevant model defining the role of flexion. Spine (Phila Pa 1976) 34:2288-2296

34. Wade KR, Robertson PA, Broom ND (2011) A fresh look at the nucleus-endplate region: new evidence for significant structural integration. Eur Spine J 20:1225-1232

35. Wade KR, Robertson PA, Broom ND (2012) On how nucleus-endplate integration is achieved at the fibrillar level in the ovine lumbar disc. J Anat 221:39-46

36. Wade KR, Robertson PA, Broom ND (2012) On the extent and nature of nucleus-annulus integration. Spine (Phila Pa 1976) 37:1826-1833

37. Wade KR, Robertson PA, Broom ND (2014) Influence of maturity on nucleus-endplate integration in the ovine lumbar spine. Eur Spine J 23:732-744

38. Wade KR, Robertson PA, Thambyah A, Broom ND (2015) "Surprise" Loading in Flexion Increases the Risk of Disc Herniation Due to Annulus-Endplate Junction Failure: A Mechanical and Microstructural Investigation. Spine (Phila Pa 1976) 40:891-901

39. Wang Y, Battie MC, Videman T (2012) A morphological study of lumbar vertebral endplates: radiographic, visual and digital measurements . Eur Spine J 21:2316-2323

40. Wang Y, Videman T, Battie MC (2013) Morphometrics and lesions of vertebral end plates are associated with lumbar disc degeneration: evidence from cadaveric spines. J Bone Joint Surg Am 95:e26

41. Yu J, Schollum ML, Wade KR, Broom ND, Urban JP (2015) A Detailed Examination of the Elastic Network Leads to a New Understanding of Annulus Fibrosus Organisation. Spine (Phila Pa 1976)

42. Yu J, Winlove PC, Roberts S, Urban JP (2002) Elastic fibre organization in the intervertebral discs of the bovine tail. J Anat 201:465-475

43. Zehra U, Robson-Brown K, Adams MA, Dolan P (2015) Porosity and Thickness of the Vertebral Endplate Depend on Local Mechanical Loading. Spine (Phila Pa 1976) 40:1173-1180

Figures and figure legends

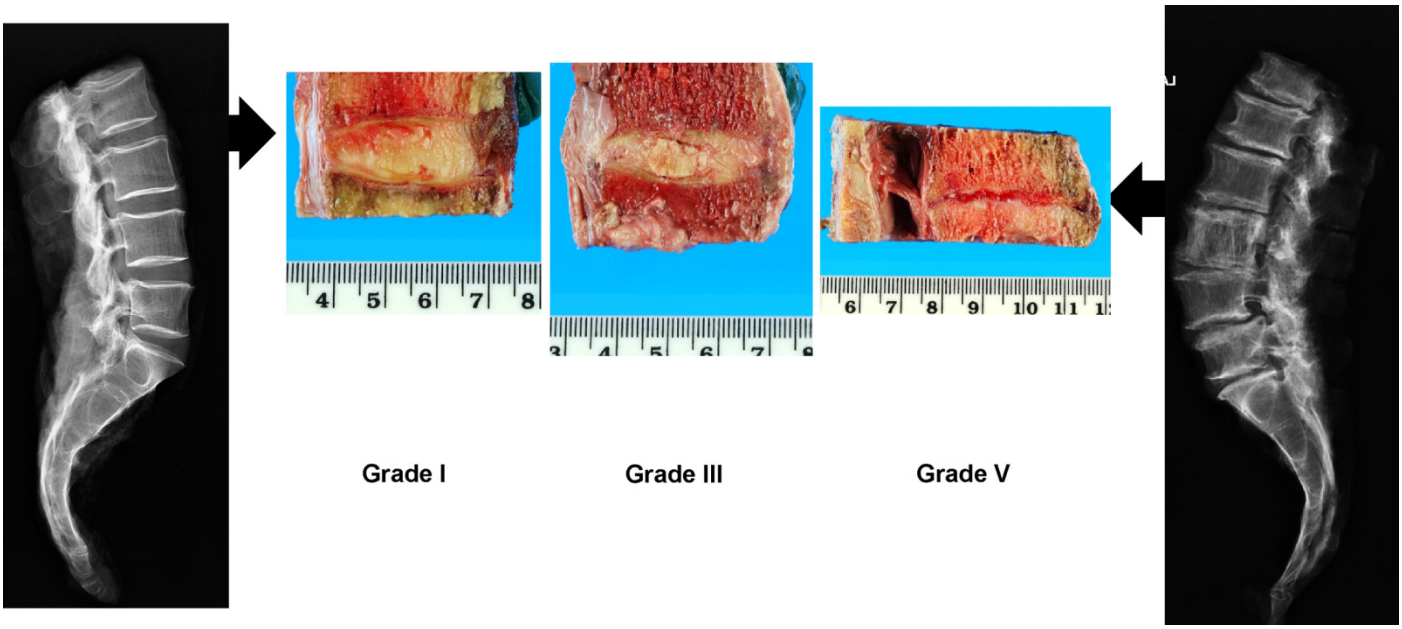

Fig. 1 Photographs and corresponding X-rays from differently graded (according to Pfirrmann Score of MRIs) motion segments used for microscopic analysis in this study

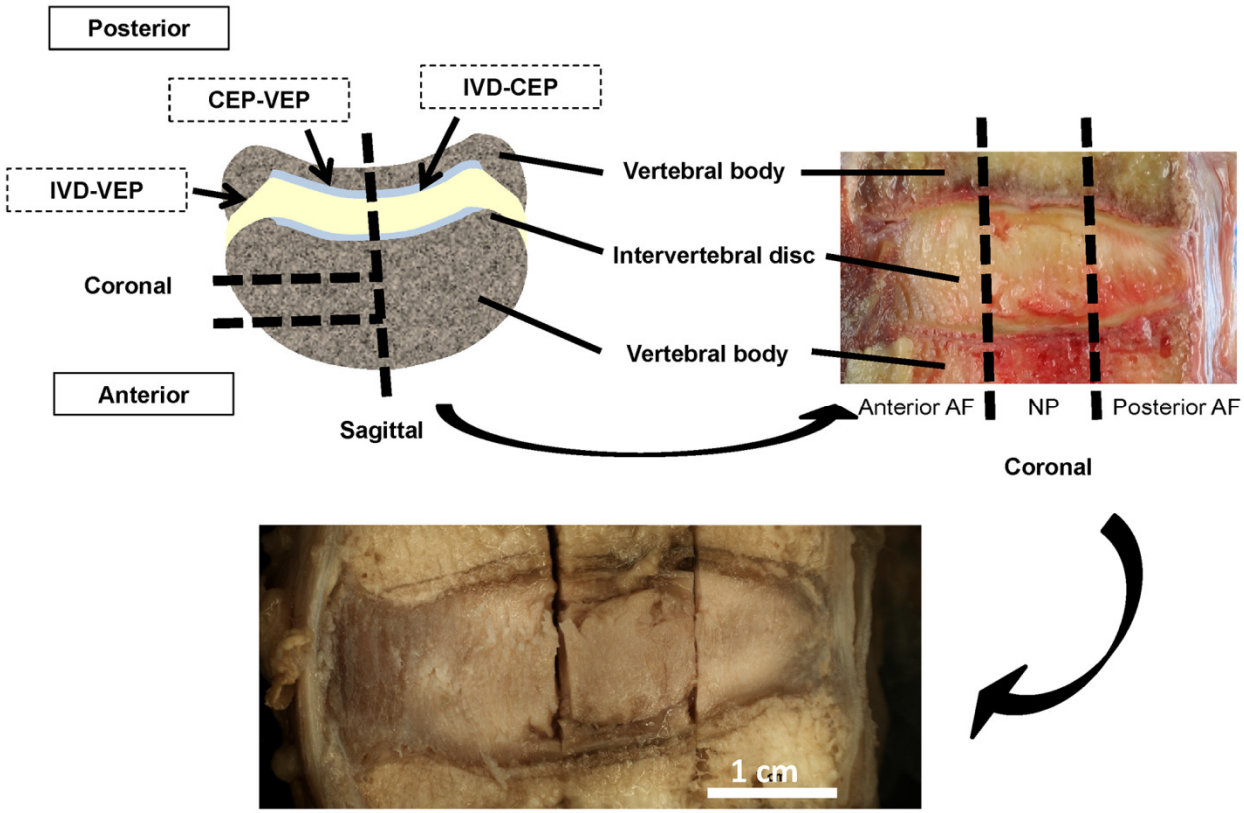

Fig. 2 Scheme for preparation of motion segments containing the anterior annulus fibrosus (AF), nucleus pulposus (NP) or posterior AF

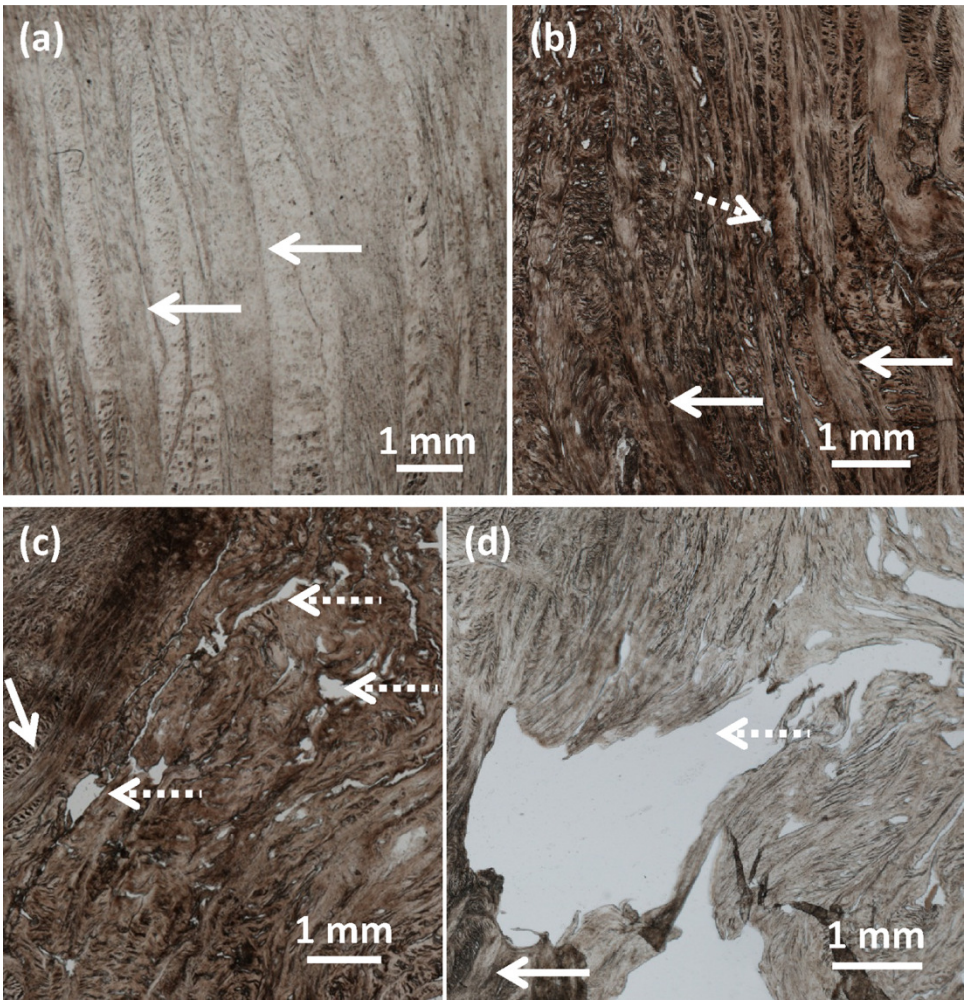

Fig. 3 Standard light microscopy images illustrating the different levels of disruption found within the annulus fibrosus (AF) described as (a) none; (b) minor; (c) moderate and (d) major that were scored from 1 to 4 respectively. Solid arrows show normal lamellae structure whereas dashed arrows highlight areas where the lamellae organisation has been disrupted and connectivity lost

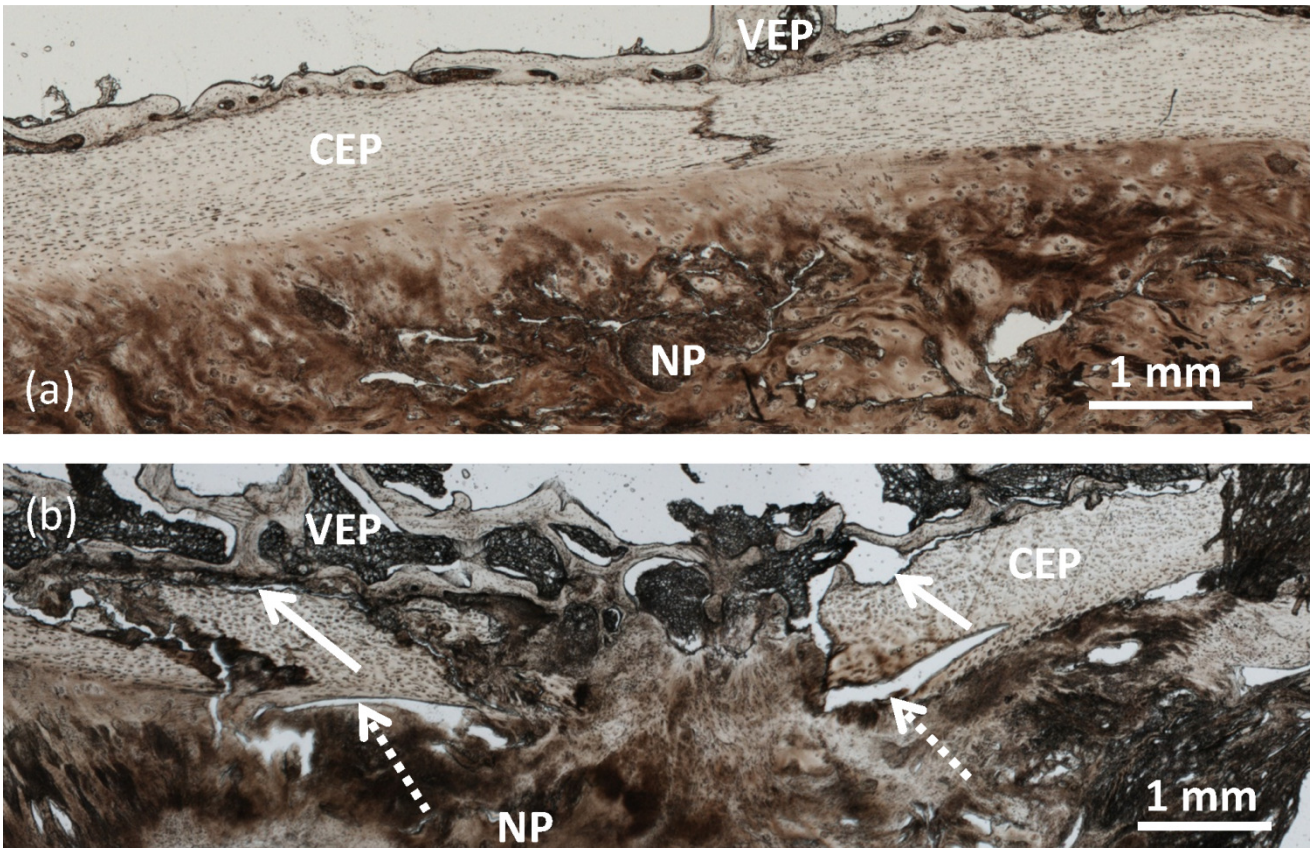

Fig. 4 Light microscopy images of human specimens showing (a) good attachment at the nucleus pulposus (NP)-cartilage endplate (CEP) and CEP-vertebral endplate (VEP) interfaces from a Pfirrmann grade I specimen and (b) detachment at the NP-CEP (dashed arrows) and CEP-VEP (solid arrows) interfaces from a Pfirrmann grade V specimen

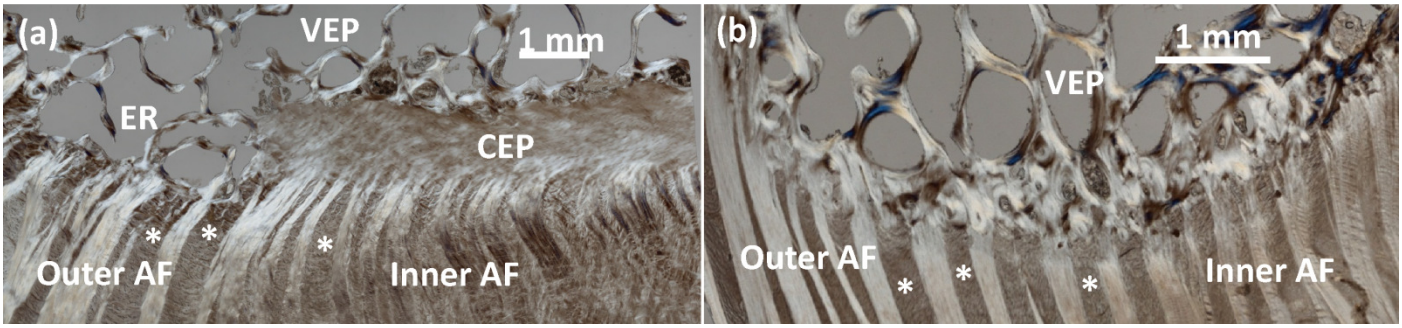

Fig. 5 Overall structure at the lumbar spine annulus fibrosus (AF)-vertebra interface in (a) human Pfirrmann grade I and (b) ovine specimen (ER = epiphyseal ring; CEP = cartilage endplate; VEP = vertebral endplate) as viewed by DIC microscopy with a few of the in-plane lamellae highlighted (*)

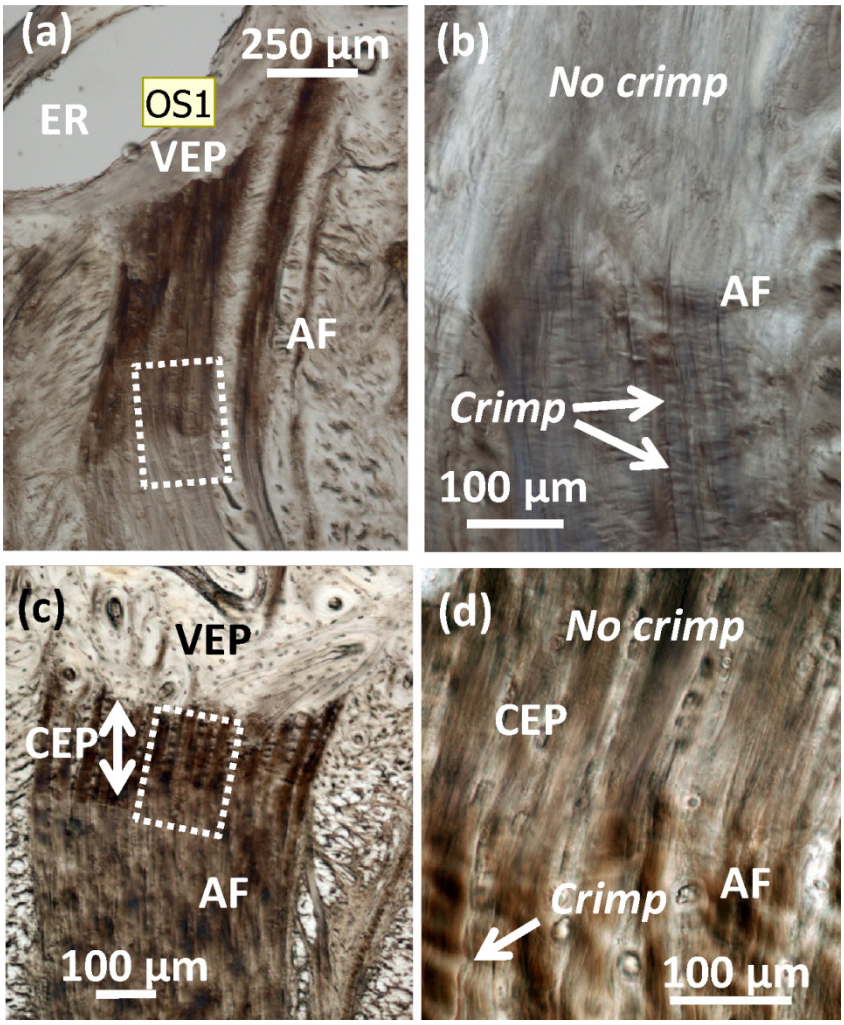

Fig. 6 DIC microscopy images of annulus fibrosus (AF) fibres in (a) human Pfirrmann grade I specimen at the epiphyseal ring (ER) attaching directly to the vertebral endplate (VEP) with change in crimp (wave-like pattern in collagen) to no crimp (collagen appears smooth) at approximately 600 µm below the VEP (boxed area) shown at a higher magnification in (b) where appearance of crimp is associated with a darker optical density (OD) whilst no crimp is associated with a lighter OD. (c) The AF-cartilage endplate (CEP) and CEP-VEP junctions in sheep [29] illustrating a change from crimp to no crimp at the AF-CEP interface (boxed area) shown at a higher magnification in (d). Double headed arrow denotes CEP depth whilst solid arrows highlight the presence of crimp

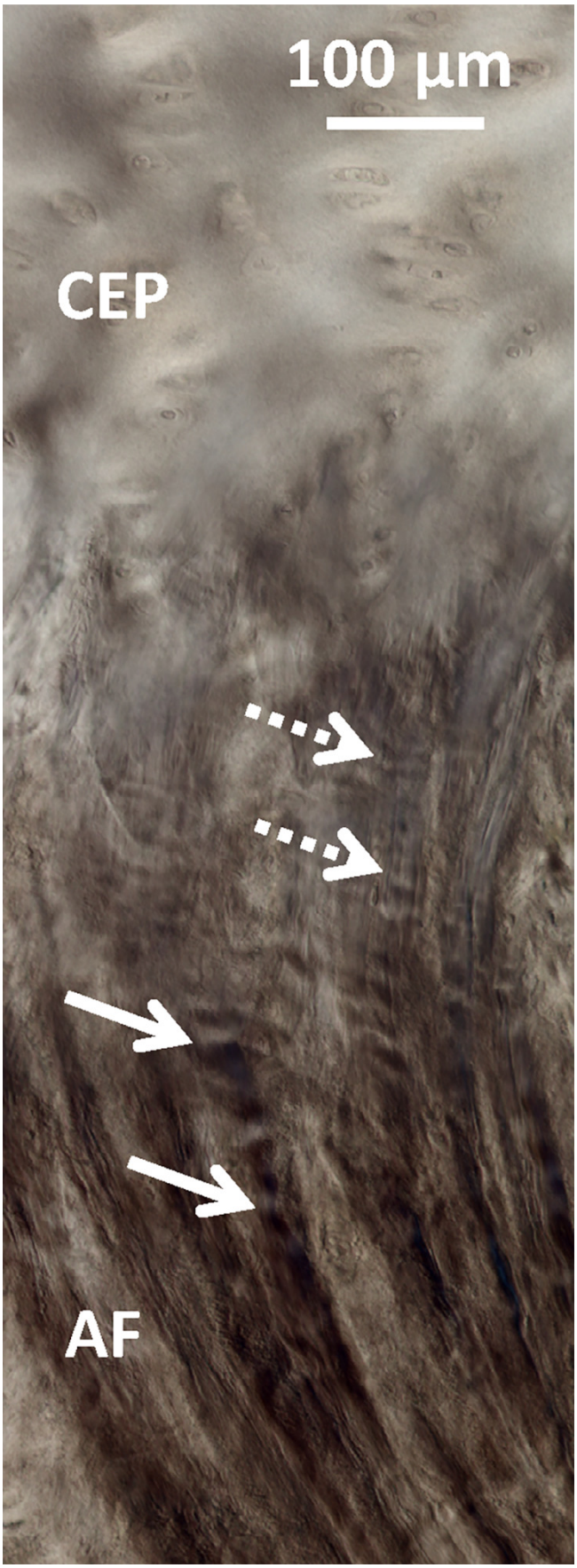
100 µm
CEP
AF

Fig. 7 DIC microscopy image of annulus fibrosus (AF) fibres prior to entering the cartilage endplate (CEP) of a Pfirrmann grade I human IVD where a change in the appearance of crimp from wider (solid arrow) to a finer morphology (dotted arrow) was observed

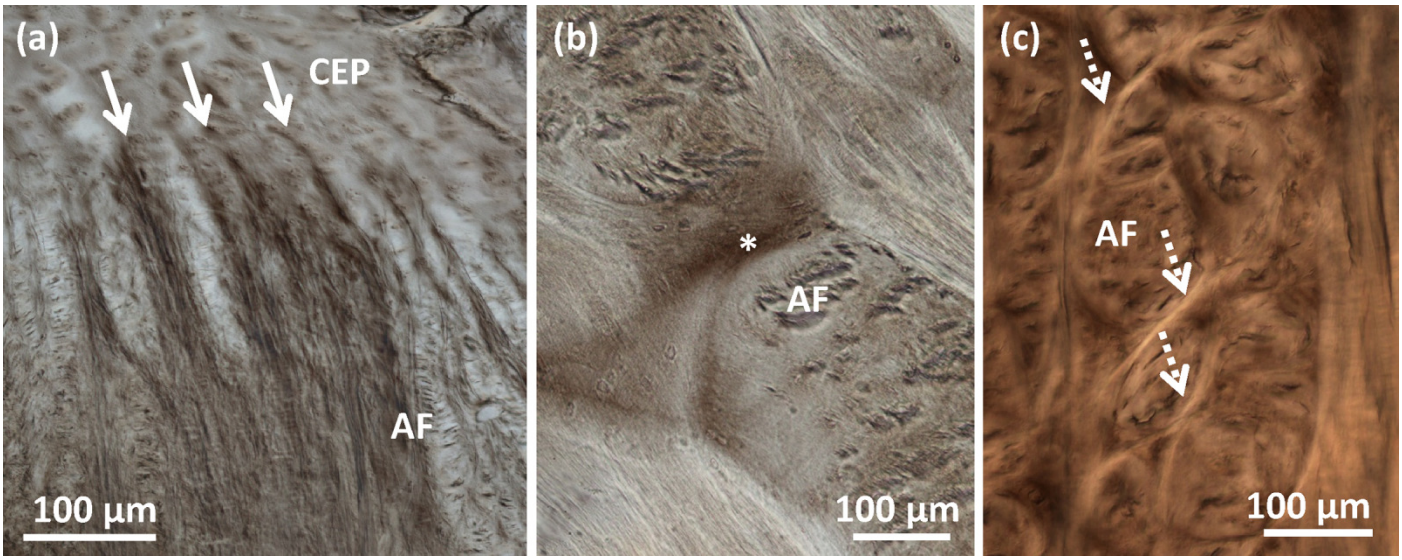

Fig. 8 DIC microscopy images of a Pfirrmann grade I IVD illustrating (a) 'branching' of fibres from an annulus fibrosus (AF) lamella (solid arrows) on entering the cartilage endplate (CEP), (b) a trans-lamellar bridge (*) within the AF and (c) a cross-section of an AF lamella showing areas (dotted arrow) where collagen fibres appear to be ensheathed within a bundle (compartmentalisation)

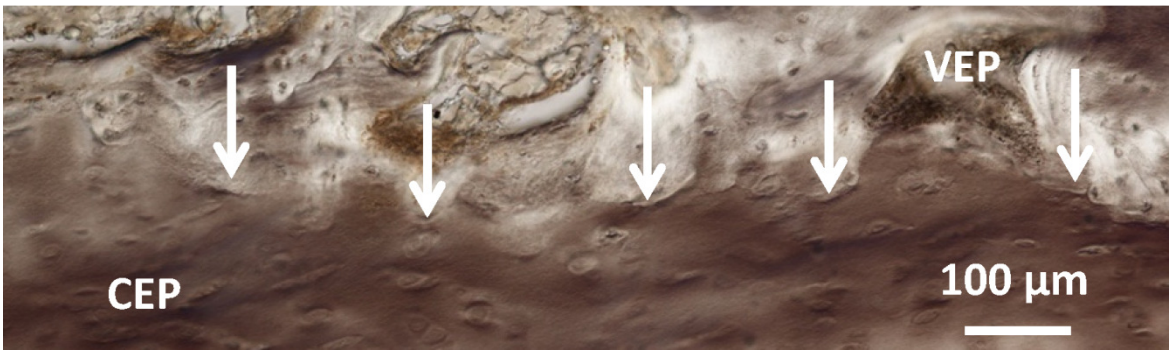

Fig. 9 DIC microscopy image of the cartilage endplate (CEP)-vertebral endplate (VEP) interface in a Pfirrmann grade I human motion segment with solid arrows indicating where the junction occurs

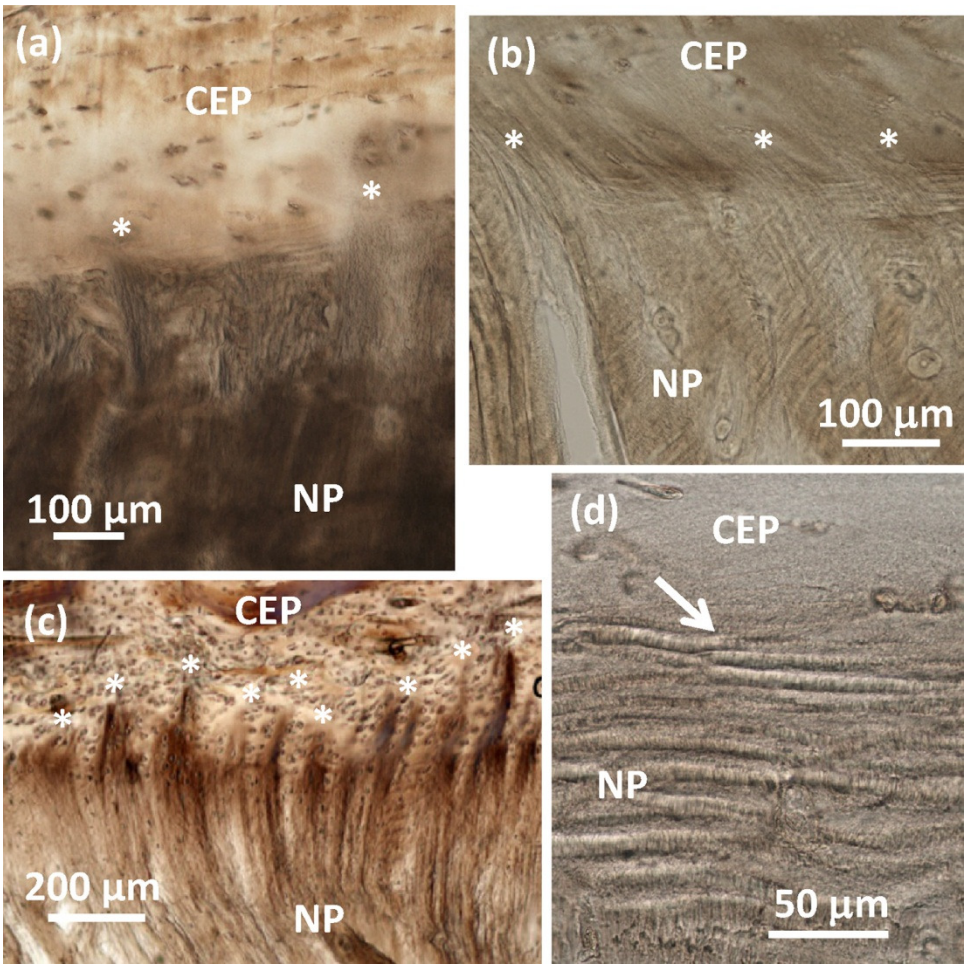

Fig. 10 DIC microscopy images of the nucleus pulposus (NP)-cartilage endplate (CEP) interface in (a) human Pfirrmann Grade I, (b) human Pfirrmann Grade III and (c) ovine specimen [35] with the presence of nodal insertions (*) as described by Wade *et al* [34], [35] being noted. (d) Illustrates the 'wave-like' morphology (solid arrow) of the NP matrix in a human Grade III specimen prior to entering the CEP

Table 1. Summary of Pfirrmann grading and degenerative changes observed from MRIs of the motion segments used in this study

Pfirrmann Grade [24]	Spinal Level	Disc narrowing	Annular tears	Disc bulging		Foraminal stenosis	Endplate defects	
				Ant	Post		Cranial	Caudal
I	L1-2	0	0	0	0	0	0	0
I	L2-3	0	0	0	0	0	0	0
III	L1-2	0	0	0	0	0	0	2
III	L2-3	0	1	1	1	0	0	0
III	L2-3	0	0	0	0	0	0	0
III	L3-4	0	0	0	0	0	0	0
III	L3-4	0	0	2	1	0	3	0
III	L3-4	0	1	0	0	0	0	0
IV	L4-5	1	0	0	1	0	0	0
V	L2-3	3	0	2	1	1	3	3

*Scoring: Disc narrowing (**0** = normal disc height; **1** = slight disc narrowing; **3** = endplates almost in contact); Annular Tears (**0** = absent; **1** = present); Anterior (Ant) & Posterior (Post) bulging (**0** = normal contour of disc <0.5 mm; **1** = slight (0.5-2.5 mm); **2** = moderate (>2.5 mm)); Foraminal stenosis (**0** = absent; **1** = mild); Endplate defects (**0** = absent; **2** = moderate defect (5-10 mm); **3** = severe defect (>10 mm))*

Table 2. Percentage detachment at the interfaces between the intervertebral disc and the vertebral bodies

		Detachment (%) between structures										
Specimen		Anterior AF			Nucleus Pulposus				Posterior AF			Overall average detachment (%) for each motion segment
					Cranial		Caudal					
Pfirrmann Grade	Spinal Level	AF-VEP	CEP-VEP	AF-CEP	CEP-VEP	NP-CEP	CEP-VEP	NP-CEP	AF-CEP	CEP-VEP	AF-VEP	
I	L1-2	0	0	0	0	0	0	0	n/a	n/a	n/a	0
I	L2-3	0	0	0	3	6	15	14	0	0	0	4
III	L1-2	0	90	0	18	20	Very disorganised		0	80	17	28
III	L2-3	3	46	0	9	30	21	3	12	19	0	14
III	L2-3	0	5	0	7	22	52	9	0	0	8	10
III	L3-4	36	1	5	100	0	21	0	3	11	5	18
III	L3-4	15	72	11	58	1	23	0	0	100	0	28
III	L3-4	0	n/a	0	n/a	n/a	7	2	Very disorganised			2
IV	L4-5	0	0	0	50	54	88	6	0	15	0	21
V	L2-3	Impossible to section			32	24	Very disorganised		Impossible to section			28
Average detachment (%) for all motion segments		**6**	**27**	**2**	**31**	**17**	**28**	**4**	**2**	**32**	**4**	
No. of samples with any detachment/total no. assessed		**3/9**	**5/8**	**2/9**	**8/9**	**7/9**	**7/8**	**5/8**	**2/7**	**5/7**	**3/7**	